Real Time Gas Quantification Using Thermal Hyperspectral Imaging: Ground and Airborne Applications

Pierre-Yves Foucher, Stéphanie Doz
ONERA, 2 av. Edouard Belin, 31400 Toulouse
FRANCE

Pierre-yves.foucher@onera.fr, Stephanie.doz@onera.fr

ABSTRACT

Whether for environmental or industrial applications, infrared hyperspectral technology is an efficient tool for studying and monitoring gas leaks. But now users need to access to real-time gas leak quantification mapping. In this purpose, several gas tests campaign has been conducted since 2015 in order to validate our algorithms for visualizing and quantifying gas plumes for different kind of gas in a very large range of flow rate (0.5g/s up to 250g/s) from hyperspectral infrared cameras in particular using TELOPS technology. In this paper, we present recent results from real time ground and airborne quantification during different hyperspectral campaigns. In particular during the NAOMI project in collaboration with TOTAL, hundreds of controlled methane leakages tests have been fulfilled. The real time algorithm IMGSPEC developed by ONERA shows a real good agreement with ground truth in term of gas flow rate. Then, airborne campaign results show the developed quantification algorithm coupling with airborne TelopsHyper-Cam system (from 600m to 1500m) provides real-time quantitative map (ppm.m), estimation of local concentration (ppm) and leakage flow rate with associated uncertainties. We finally show IMGSPEC application to other kindof gas as Acetone or Methanol.

1.0 INTRODUCTION

Gas leaks present obvious health and safety risks. The need for a reliable and cost-efficient gas detection system is of prime importance especially when security threatening situations like gas leaks and emissions occur. Quantification of the gas flux emanating from the leaks may help the incident response team to take actions. In this regard, infrared remote sensing technology offers many benefits over traditional gas detection systems as it allows monitoring and imaging of the incident scene from a safe location. The sensor can be located at distances ranging from tens of meters to several kilometres from the scene, avoiding the need to access restricted and potentially dangerous zones.
However, emissions flow estimation remains poor at a high spatial resolution over heterogeneous scenes or is time consuming and not suitable with the need of emergency response in case of gas leak detection. Gas plumes have mostly a small extent and require a high spatial resolution imagery which can be achieved with existing LWIR airborne hyperspectral systems [1][2][3][4] or from ground hyperspectral systems [5][6][7][8]. In the LWIR domain, emission of gas is not neglected and brightness temperature difference between the ground and the plume will be the key parameter for detection and quantitative retrieval. Existing approaches which use the spatial and spectral information to characterize gas plume can be divided into two categories: endmember decomposition techniques to estimate the background properties and trace element detection [10] or quantification methods based on an estimation of all the radiative terms (background, atmosphere and gas) .The background uncertainties are the major sources of incertitude in gas quantification. Most of quantitative algorithms aim to estimate ground and gas properties as the same time use iterative minimization between a direct radiative transfer model (RTM) calculation and measurements, the main issue is these methods are time consuming and need to implement a RTM inside the algorithm[4][5][8]. The method used here based on two independent steps, one for background estimation and another for gas concentration estimation is very fast and do not use RTM calculation[3][9].

2.0 REAL TIME METHODOLOGY

The method presented here has been implemented in the IMGSPEC code developed by Onera for several years. The IMGSPEC method computes concentration without iterations allowing real-time processing. The main output of the algorithm is the column path concentration map of the gas plume (ppm.m). This data can however hardly be validated because the available ground truths are mainly flow data and not integrated concentration data. Therefore, an additional step is required to estimate the flow rate. Among the possible methods, we mainly use an instantaneous method requiring wind data. However, in some cases (Cf. §3.3 and §4), wind speed may be deducted from acquired data.

1·1·1·1 Principe

The quantification algorithm is based on the resolution of the physical equation of the camera input radiance. Considering R_{gas} the input radiance measured during an acquisition with gas emission and R_{ref} the associated reference radiance with no gas. Equations of R_{gas} and R_{ref} can be written for every band and every pixel as the following equation:

$$R_{gas} = \tau_{gas}.\tau_{atm}.R_{bkg} + \tau_{atm}.\left(1-\tau_{gas}\right).B\left(T_{gas}\right) + L_{atm}$$

$$R_{ref} = \tau_{atm}.R_{bkg} + R_{atm}$$

R_{bkg}	*radiance emitted by the background*
τ_{gas}	*gas transmission*
τ_{atm}	*air column transmission*
$\left(1-\tau_{gas}\right).B\left(T_{gas}\right)$	*radiance emitted by gas depending on its temperature T_{gas} and on its emissivity $\left(1-\tau_{gas}\right)$*
R_{atm}	*radiance emitted by the air column*

The gas transmission depends on the gas concentration and may be calculated using this equation.

$$\tau_{gas} = 1 + \frac{R_{gas} - R_{ref}}{\left(R_{ref} - R_{atm} - \tau_{atm}.B\left(T_{gas}\right)\right)}$$

To solve this equation several assumptions are made because R_{ref}, R_{atm}, T_{gas}, τ_{atm} are not directly known.

T_{gas} is considered equal to T_{atm} at the ground level. Even if the gas source may be colder or warmer than atmosphere, as it dissipates the gas is quickly released at surrounding temperature.

R_{ref} corresponds to the radiance of the scene without gas. Most of gas detection systems need an acquisition of the scene before the gas leak occurs. But such acquisition is not always available especially when the sensor is in motion. IMGSPEC algorithm contains a step of background signal reconstruction and can be run with airborne acquisition for instance. The methodology used is based on the CSB algorithm [3][6].

Finally, the calculation of R_{atm} and τ_{atm} depends logically on the type of acquisition, ground or airborne.

Ground case:

In this case, $Ratm = (1 - \tau_{atm}).B(T_{atm})$. T_{atm} is easily known from saturated water vapor channels and τ_{atm} is calculated from a water vapor concentration delivered by a meteorological station and estimated distance of the target. Thus, in the ground case, considering T_{gas} equals to T_{atm} we can estimate than:

$$\tau_{gas} = 1 + \frac{R_{gas} - R_{ref}}{\left(R_{ref} - B(T_{gas})\right)}$$

Airborne case:

Here, estimation of τ_{atm} et R_{atm} need knowledge of vertical profile of atmospheric gases (mainly water vapor) and temperature from the ground to the airborne. In order to have a fast estimation of these variables we use a calculation inspired by ISAC method [12][13][14].

2.2 Flow rate estimation

Flow rate of the gas plume is computed estimating the quantity of the gas transported by the wind in one second. The concentration map in output of IMGSPEC is an instantaneous state of the gas plume. Its shape and concentration depend on the flow rate and the wind speed. Assuming the wind direction is orthogonal to the camera viewing direction, the flow rate can be computed as the product of the wind speed and a 1-m width "slice" of gas.

$$f = m_{gas\_1m} \times s_{wind}$$

m	*mass of the plume for a 1 meter width "slice" (unit g/m)*
s	*wind speed (unit m/sec) at the perpendicular direction of the camera viewing direction*
f	*flow rate (g/sec)*

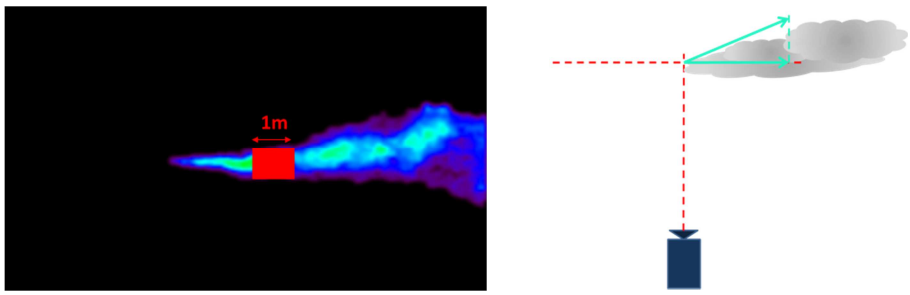

Figure 2-1: Flow rate is estimated using concentration map (left) and the transversal wind speed (right)

The wind measurement integration time of meteorological stations may be about few seconds. Thus, the wind state at the acquisition time is never exactly known. More the wind direction changes frequently and the orthogonal condition is never respected. Therefore, flow rate estimation method does not provide a precise result. However, a time average of these estimates was observed as a good estimation of the real flow rate.

3.0 GROUND RESULTS

3.1 Case of Methane

3.1.1 Test site and sensors

In the past few years (2015, 2017, 2018), three test campaigns have been occur on the gas test platform of Total in Lacq, France. This platform is equipped with controlled gas release system in order to be able to simulate a leak accident on an industrial environment. Hundreds of releases were made during these campaigns, mainly of methane but also of SF6 and ethylene. Flow rates varied between 0.3 g/s and 300 g/s.

Hyperspectral cameras were settled at a distance of about 100 m from the emission points. During these campaigns several cameras were used belonging to two main families of TELOPS HYPER-CAM: Very Long Wave Hyper-cam (VLW-HC) and Methane Hypercam (Meth-HC). The main difference between them lies in the spectral range: 7.7-11.7 µm for VLW-HC and 7.4-8.3 µm for Meth-HC. Spectral resolution can be adjusted between 2 cm^{-1} and 10 cm^{-1} and this will be an impact on the integration time and frame rate. A high spectral resolution is adapted to very low flow rate leaks. And a high frame rate is useful to study the spatial variations of the plume. Finally 5 cm^{-1} spectral resolution has been chosen as a good comprise to study maximum cases.

For these ground campaigns, HYPERCAM cameras were used thanks to our partnership with TELOPS and IMGPSEC algorithm was running in real time inside HYPERCAM own computer. However the post processing algorithm IMGSPEC is not exclusively devoted to these cameras and can be run with any kind of thermal hyperspectral camera. More, the algorithm can be used for any gas whose signature corresponds to the spectral band of the used camera.

3.1.2 Quantitative results

As described on the methodology section, a part of the processing consists in reconstruction of the reference signal from an acquisition containing gas. The figure 3-1 shows an example of the results of the reference reconstruction. The left image is an extract of the acquisition during a release at 1303cm^{-1} in brightness temperature. At this wavenumber the absorption of methane is maximum. The gas plume can be distinguished as the dark area spreading from the centre of the image to the right part. The central image is the reconstructed reference; the gas plume does not appear. On the left side, the image is an extract at 1303 cm^{-1} of an acquisition of the scene just before the gas release. Three vertical profiles are extracted from these images to be compared.

Figure 3-1: Acquired data with gas (left), reconstructed reference (centre), acquired data with gas (right); all at 1303cm^{-1}

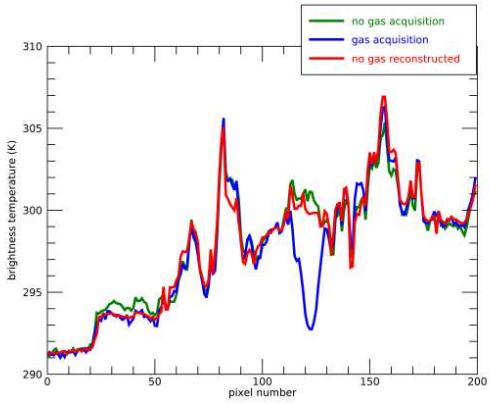

Figure 3-2: Vertical profiles extracted from images of figure 3-1, gas absorption is around the pixel 120

The green and the blue curves, extracted directly from acquisitions, are very similar because the acquisition times are very close. The difference is around the pixel 120, corresponding to the gas position. Gas temperature is colder than background; this is why the blue curve decreases until 293 Kelvin. The red curve corresponds to the reconstructed signal, close to the green curve (no gas acquisition).

The next figure presents the results of three tests at 1 g/sec, 10 g/sec and 85 g/sec. First, concentration map (in color) has been overlap to the scene acquisition (in grey). The color scale is relative to the gas concentration in ppm.m and is common to the three tests. Below, the graphs show the temporal flow rate computed for every acquisition (1 acquisition every 4 sec.) associated to an error bar.

For these extracts, plume is fully detected excepted in the sky area. Indeed, there is no thermal contrast between gas and background, thus detection is no possible. On the heart of the plumes, concentration levels are very dependent on the flow rate.

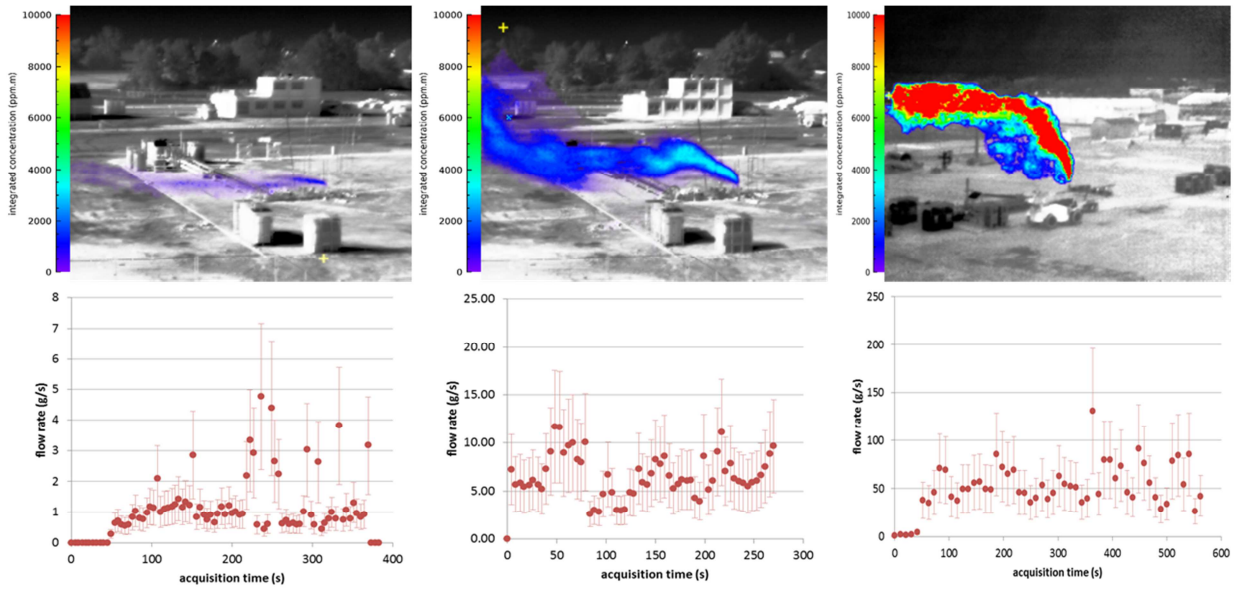

Figure 3-3: Integrated concentration map and temporal flow estimate for 1 g/sec (left), 10 g/sec (centre) and 100 g/sec (right) tests

The estimated flow rate incertitude is mainly due to the wind speed incertitude which is about 50%. In spite of this high rate, order of magnitude is respected. For industrial applications such as accident prevention, more

accuracy is not required.

The next figure gathers the results of 2018 campaign tests between 0.5 g/sec and 10 g/sec. These graphs compare flow rate estimate with real flow rate for two cameras and shows a global incertitude of 50% (mainly wind incertitude).

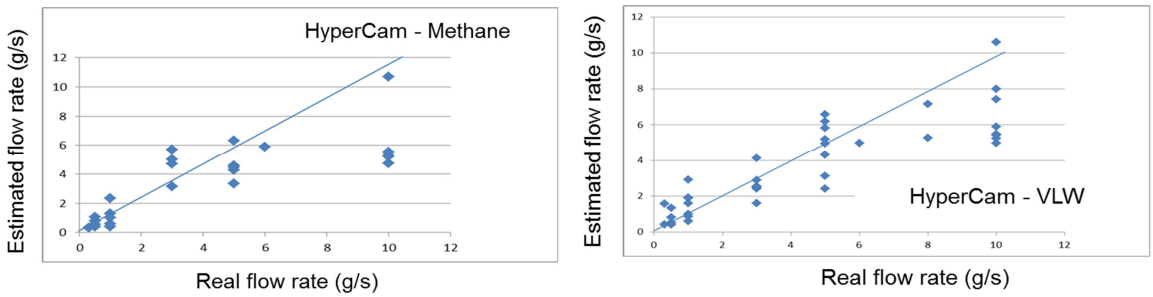

Figure 3-4: Comparison between real flow rate and flow rate estimate for 2018 campaign tests.

From concentration maps, other data can be deducted. As linear concentration is know on each pixel, sum of pixels leads to the total mass of the gas plume (using the massive density of the gas) and thus, its explosiveness rate. More, with spatial symmetry assumptions, concentration on local points may be deducted (see §4.1).

3.3 Case of other trace gases

Methane is a good candidate for validation of IMGSPEC ground algorithm because absorption spectrum is not very strong and well mixed with water vapour (see figure 3-5). But the algorithm has also been used for other kind of gas with absorption in the LWIR spectral domain. We present here examples corresponding to Ethylene and MTBE from HyperCam VLW acquisition in an industrial site in figure 3-6.

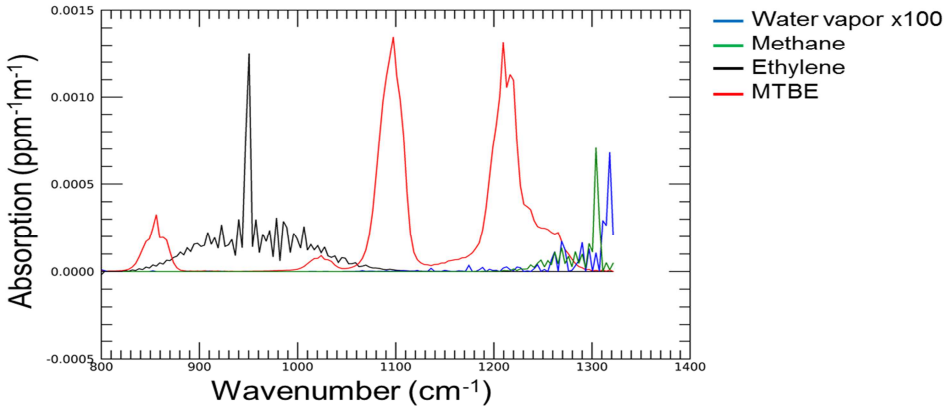

Figure 3-5: Gases spectral absorptions

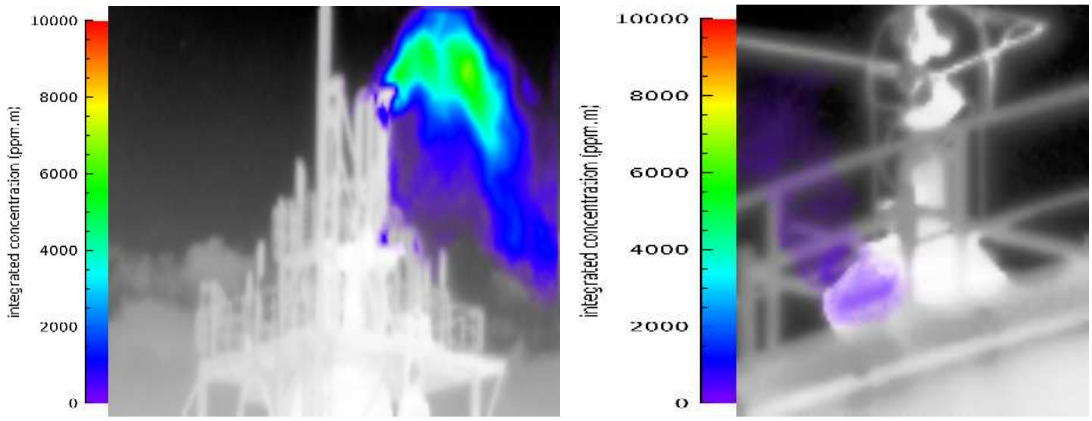

Figure 3-6: Left Ethylene quantification map, Right: MTBE quantification map

Parallel to the tasks described in the previous section when wind is very turbulent or known with a large uncertainty, the raw interferogram images can be processed in order to extract a velocity map of the plume (i.e. both amount and direction). To achieve that goal, a dedicated algorithm from TELOPS processes the entire sequence of acquired data cubes in order to estimate the velocity of the turbulent gaseous emissions [5]. The velocity in the plume is finally used to convert the global column density into a mass flow rate.

4.0 AIRBORNE RESULTS

4.1 Gas quantification from Hyper-Cam-VLW instrument

Airborne acquisition were achieved by TELOPS in summer 2017 over urban area (Quebec City) using the target mode (8 acquisitions over the same area during the same line of flight) over release of acetone and methanol. The altitude of flight is 700m and the pixel size is 1m.

In this configuration, the Telops Hyper-Cam is installed on a stabilization platform equipped with a global positioning system (GPS) and inertial motion unit (IMU). In a FTS imaging system, signal modulation is achieved using a Michelson interferometer. Acquiring a full interferogram typically lasts about one second at $5cm^{-1}$ resolution. Therefore, an image motion compensation mirror uses GPS/IMU data to compensate efficiently for the aircraft movements during data acquisition. The typical NESR is 15 $nW/cm^2/sr/cm^{-1}$.

The figure 4-1 shows the case of acetone evaporating from a plate. The different images correspond to the concentration map (ppm.m) for each acquisition from the target mode (temporal shift of 0.7s). The maximum of concentration is around 650 ppm.m, with a longitudinal extent of 25m and a cross wind extent of 10m at the centre of the plume. The mean total mass of acetone seen in the plume is 11 g (standard deviation of 0.9 g). Supposing that the vertical extent of the plume is similar to the cross wind extent we can estimate that the local concentration in the centre of the plume is around 65 ppm. The mean linear mass (g/m) estimated in the centre of the plume is 2.1 g/m (standard deviation of 0.5 g/m). By observing the spatial displacement of the plume, we can then estimate the gas velocity. From the first image to the last one the maximum of concentration (centre of the plume) spatial shift is estimated to 8m, the mean wind speed is estimated to be around 1.5 m/s. Corresponding estimated flow of this plume is 3.1 g/s (standard deviation of 0.8 g/s).

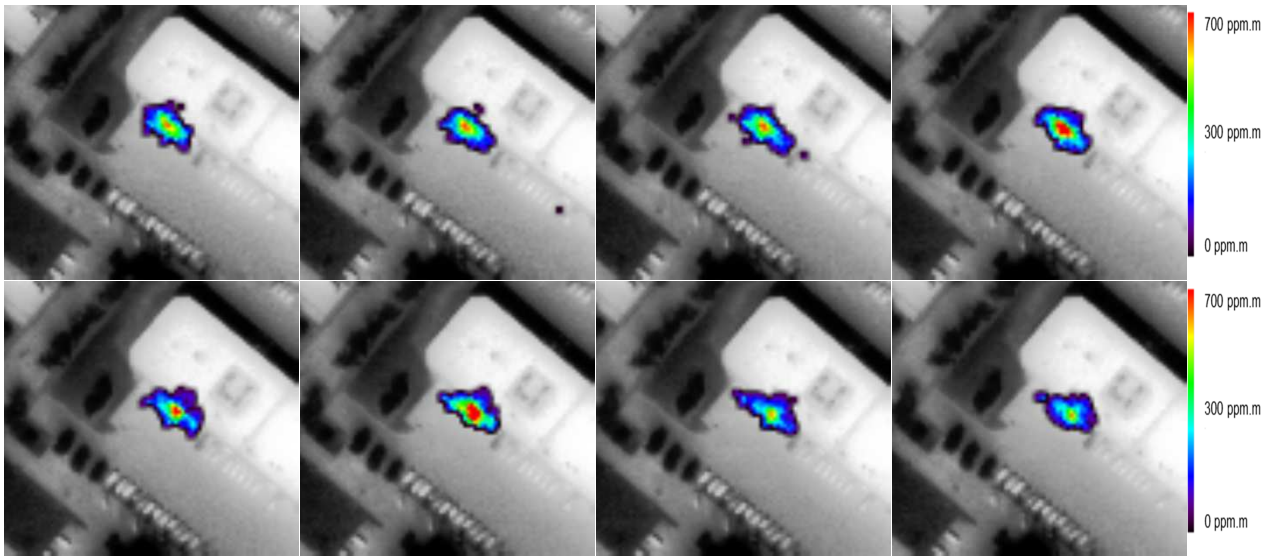

Figure 4-1: Sequence of quantitative map (ppm.m) over acetone plume using Hyper-Cam target mode.

The figure 4-2 shows same kind of result for a methanol plume evaporating in the same area (at the same time).The maximum of concentration is around 250ppm.m, with a longitudinal extent of 46m and a cross wind extent of 10m at the centre of the plume. The mean total mass of methanol seen in the plume is 17.8 g (standard deviation of 0.6 g). The mean linear mass (g/m) estimated in the centre of the plume is 1.2 g/m (standard deviation of 0.2 g/m). Supposing that the vertical extent of the plume is similar to the cross wind extent we can estimate that the local concentration in the centre of the plume is around 25 ppm. By observing the spatial displacement of the plume, we can then estimate the gas velocity. From the first image to the last one the maximum of concentration (centre of the plume) spatial shift is estimated to 8 m and the mean wind speed is estimated to be around 1.5 m/s (coherent with the wind speed estimated from acetone plume spatial shift). Corresponding estimated flow of this plume is 1.8 g/s (standard deviation of 0.3 g/s).

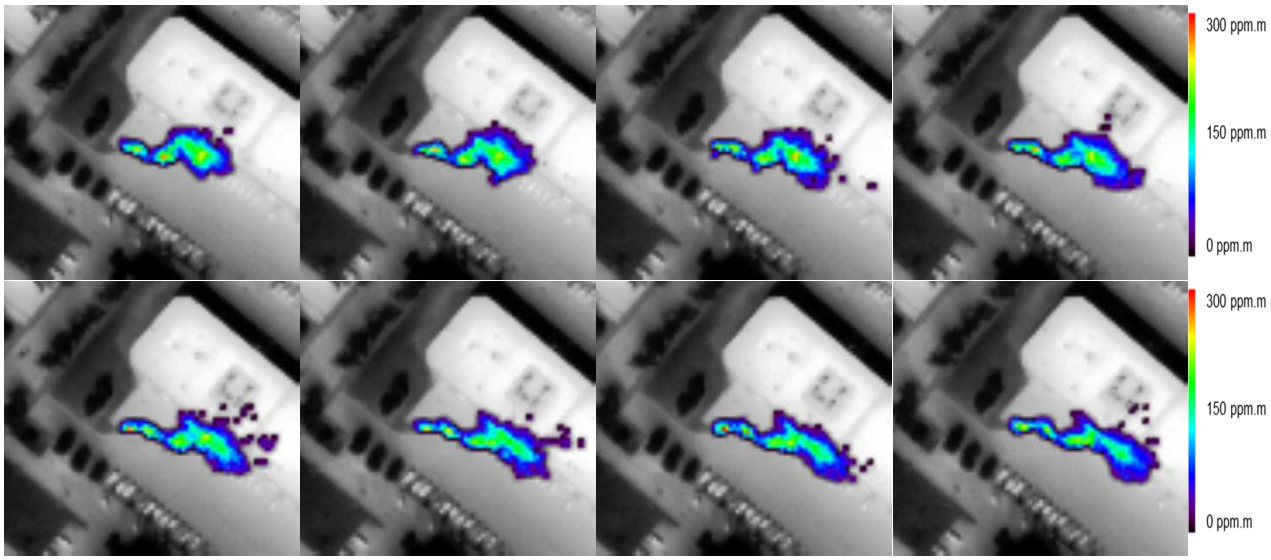

Figure 4-2: Sequence of quantitative map (ppm.m) over methanol plume using Hyper-Cam target mode.

These two gases have a high saturation vapor pressure (23kPa at 20°C for Acetone and 12kPa for methanol) which explain the high volatility and the important concentration and flow rate. Acetone maximum concentration and flow rate seems to be higher than for methanol (as the saturation vapor pressure is higher)

The difference of the saturation vapor pressure (23kPa at 20°C for Acetone and 12kPa for methanol) can explain that the flow rate seen from acetone evaporation is higher than methanol flow rate. However extent of acetone plume is lower than for methanol as strength of absorption lines in the LWIR are lower for acetone than for methanol (0.8 10^{-3} $ppm^{-1}.m^{-1}$ at 1216cm^{-1} for acetone and 1.28 10^{-3} $ppm^{-1}m^{-1}$ at 1034 cm-1 for methanol).

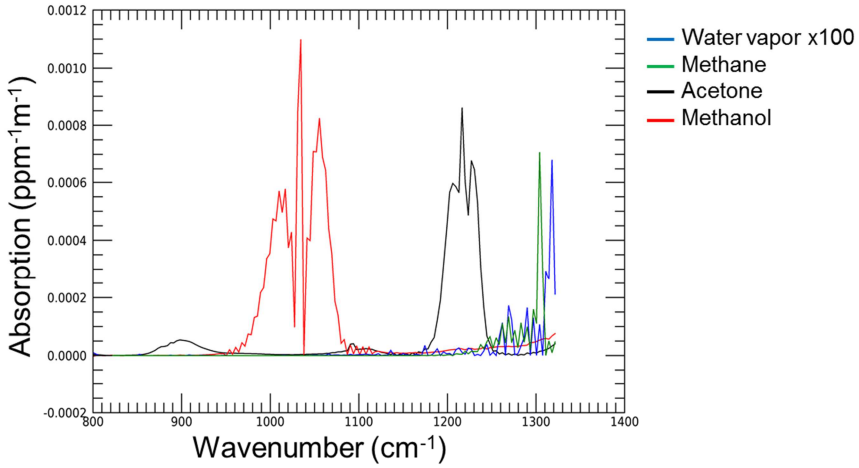

Figure 4-3: Absorption of specific gases

4.2 Gas quantification from Hyper-Cam-Methane instrument

The Telops Hyper-Cam Methane cover the7.4-8.3 µm spectral range with a typical NESR of 6 $nW/cm^2/sr/cm^{-1}$. During the 2018 experiment on the gas test platform of Total in Lacq, France, different releases from 0.5 to 300 g/s have been achieved corresponding to flight altitude from 600 to 1500 m. Examples of quantitative maps are shown in the next figure.

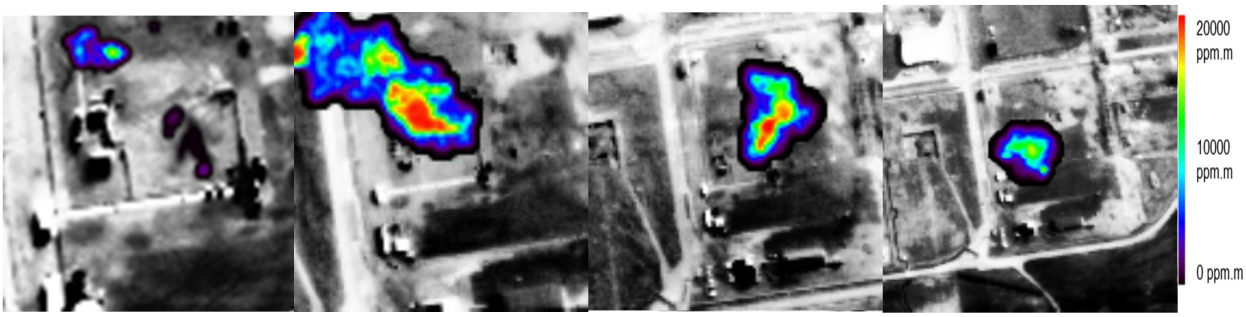

Figure 4-4: Concentration map from IMGSPEC airborne corresponding respectively (from left to right) at 1 g/s at 600m, 200 g/s at 900m, 80 g/s at 1250m and 50 g/s at 1500m.

During this campaign wind speed from a meteorological Lidar was provided in real time and used for flow rate estimation. Magnitude of estimated flow rate was in a good agreement (mean error of 50%) with real flow rate from 0.5 to 300 g/s as shown in the figure 4-5.

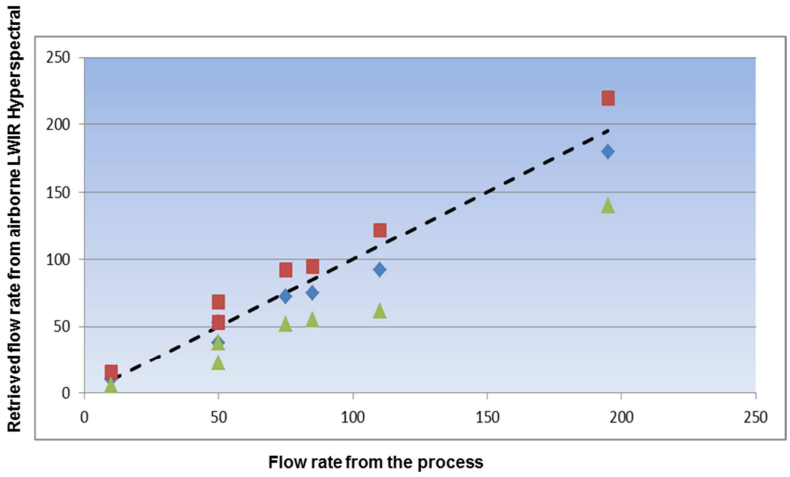

Figure 4-5: Comparison between estimated flow rate (blue diamond) and real flow rate (dotted dark line). Red and green dots represent the standard deviation of the uncertainty of retrieval.

5.0 CONCLUSIONS

IMGSPEC is a fast quantitative algorithm estimating column path concentration from ground or airborne LWIR thermal hyperspectral data. This algorithm also provides plume propagation direction, linear mass in the cross wind direction, total mass and an estimation of the local concentration under Gaussian distribution hypothesis. Accuracy of the method in term of column path concentration coupling with wind estimation provides real time quantitative images and an estimation of leak flow rate. An exhaustive validation in the case of methane with many experiments (more than hundreds tests over three different campaigns) have been achieved and have shown a good agreement in term of retrieved magnitude of the flow rate (mean error around 50%). We have shown that this algorithm can be applied to provide flow rates for any gas with signature in the LWIR domain (if absorption lines are strong enough relatively to the amount of gas). As the main issue is to provide an accurate estimation of the wind speed associated to the plume, coupling IMGSPEC with instrument which can provide directly plume velocity (using a frame rate at least of 1hz) is a great advantage.

6.0 ACKNOWLEDGEMENTS

We would like to thank the entire Telops team with whom we work. Our successful collaboration has allowed us to acquire hundreds of data with Hyper-Cam cameras and we hope it will continue. We also would like to thank the TADI team for their efficiency.

7.0 REFERENCES

[1] S. J. Young, "Detection and quantification of gases in industrial-stack plumes using thermal-infrared hyperspectral imaging", Aerosp. Rep. ATR-2002 (8407), vol. 1, 2002.

[2] D. M. Tratt, K.N. Buckland, J.L. Hall, P.D. Johnson, E. R. Keim, I. Leifer, K. Westberg and S. J. Young,

"Airborne visualization and quantification of discrete methane sources in the environment" , Remote Sens. Environ., 154, 74–88, 2014.

[3] R. Idoughi, T. Vidal, P-Y. Foucher, X. Briottet, 2016, "Background radiance estimation for gas plume quantification in downlooking thermal infrared Images", Journal of Spectroscopy, Hindawi Publishing Corporation, February 2016, Vol. 2016, No. 1.

[4] F L. Kuai , J. R. Worden, K-F. Li, G. C. Hulley, F. M. Hopkins, C. E.Miller, S. J. Hook, R. M. Duren, and A. D. Aubrey, " Characterization of anthropogenic methane plumes with the Hyperspectral Thermal Emission Spectrometer (HyTES): a retrieval method and error analysis", Atmos. Meas. Tech., 9, 3165–3173, 2016.

[5] P. Tremblay, "Standoff gas identification and quantification from turbulent stack plumes with an imaging Fourier-transform spectrometer". Proc. SPIE 7673, 76730H, 2010.

[6] S. Savary "Standoff identification and quantification of flare emissions using infrared hyperspectral imaging". Proc. SPIE 8024, 880240T, 2011.

[7] S. E. Golowich and D. G. Manolakis, "Cramer-Rao bounds for long-wave infrared gaseous plume quantification," Opt. Eng., vol. 53, no. 2, p. 021109, 2014.

[8] M. Gafalk, G. Olofsson, P. Crill and D. Bastviken "Making methane visible", Nature Climate Change volume 6, pages 426–430, 2016.

[9] S. Doz, P.-Y.Foucher, X. Watremez, "Methane leak near real time quantification with a hyperspectral infrared camera" SPIE, Proceedings Volume 10661, Thermosense: Thermal Infrared Applications XL; 1066103, 2018. doi: 10.1117/12.2304819.

[10] C. C. Funk, J. Theiler, D. A. Roberts, C. C. Borel, "Clustering to improve matched filter detection of weak gas plumes in hyperspectral thermal imagery", IEEE transactions on geoscience and remote sensing 39, no. 7: 1410-1420, 2001.

[11] X. Watremez, N. Labat, G. Audouin, B. Lejay, X. Marcarian, D. Dubucq, A. Marblé, P-Y Foucher, L. Poutier, R. Danno, D. Elie, M. Chamberland, "Remote Detection and Flow rates Quantification of Methane Releases Using Infrared Camera Technology and 3D Reconstruction Algorithm", SPE Annual Technical Conference and Exhibition, november 2016. DOI: 10.2118/181501-MS.

[12] S. J. Young, B. R. Johnson and J. A. Hackwell, "An In-scene Method for Atmospheric Compensation of Thermal Hyperspectral Data," J. Geophys. Res. Atmospheres, Vol. 204, pp. ACH 14-1 – ACH 14-20, 2002.

[13] L. Bernstein, J. Gelbord, S. Adler-Golden, N. Guler, R. Sundberg, P. Conforti, "An improved in-scene atmospheric retrieval and correction algorithm for long-wavelength infrared hyperspectral imagery", Proc SPIE 10768, Imaging spectroscopy XXII : Applications, Sensors,and Processing, September 2018.

[14] P-Y. Foucher, S. Doz, J.P Gagnon, M. Chamberlain, X. Watremez, " Real time Airborne Gas quantification using Thermal Hyperspectral Imaging : Application to methane. ", Remote Sens, 2019 Special Issue Imaging Spectroscopy Avancements in Understanding Earth System submitted.